Research on the microstructure transformation and mechanical properties of lead alloy layer covering copper electrodes of high-capacity lead-acid batteries upon heat treatment

Doan Minh Cuong, Nguyen Thi Huong*, Dinh Van Long,
Vu Quang Hung, Nguyen Tien Manh, Vu Minh Thanh

Institute of Materials, Biology and Environment/Academy of Military Science and Technology, 17 Hoang Sam, Nghia Do, Hanoi, Vietnam.
*Corresponding author: nguyenhuong0916@gmail.com
Received 13 Apr. 2026; Revised 2 Jun. 2026; Accepted 13 Jul. 2026; Published 25 Aug. 2026.
DOI: https://doi.org/10.54939/1859-1043.j.mst.113.2026.96-103

ABSTRACT

The lead alloy layer on the copper electrodes of high-capacity lead-acid batteries is manufactured by gravity casting. In the cast state, the lead alloy layer exhibits a dendritic, unbalanced crystal structure, a high hardness of 27.9 HV, high residual internal stress, and a high resistance of 0.312 ÷ 0.420 mΩ, making it prone to microcracks and unfavourable for the battery. Through heat treatment, including quenching at 220 °C for 60 minutes followed by aging at 110 °C for 7 hours, the cast microstructure transforms into a more balanced, polygonal, axial crystal structure. The hardened phase forms, achieving an optimal hardness of 16.2 HV, and the average resistance is reduced to 0.06 mΩ, making it suitable for the manufacture of high-capacity lead-acid batteries.

Keywords: Lead-acid batteries; Electrode alloys; Microstructure; Hardness; Heat treatment.

1. INTRODUCTION

Currently, about 70 - 80% of the world's lead production is used in the battery manufacturing industry. Although many new types of batteries and accumulators have been developed, lead-acid batteries are still widely used because of their ease of production, ease of recycling, abundant raw materials, low cost, and flexibility in production, as well as their mature and reliable technology for automotive, stationary, and motive-power applications [1-3]. In the structure of a lead-acid battery, the electrode terminal serves as the physical connection point between the battery and the electrical system, conducting current to operate the equipment and, during recharging, simultaneously circulating electrons between the electrode plates during the chemical reaction. Therefore, in terms of mechanical properties, the battery electrode terminal must meet the requirements of high hardness for mechanical durability, low resistance to ensure good conductivity, and good corrosion resistance under sulfuric-acid service conditions [1-3].

High-capacity lead-acid batteries with advanced Pb-Sn-Ca alloy electrode plates are a specialised type of battery commonly used in marine propulsion systems, lifting equipment, and towing equipment. Unlike conventional lead-acid batteries (with pure lead metal electrodes), the electrodes of these high-capacity batteries are made of technical copper and coated with a Pb-Sb lead alloy. Although the electrode plates are made of Pb-Sn-Ca alloy, the cast lead alloy coating the copper electrodes is usually Pb-Sb alloy because it has good fluidity and wettability in the liquid state, making it suitable for electrode manufacturing. The combination of a technical copper core for strength and good conductivity with a Pb-Sb lead alloy outer layer for corrosion resistance is ideal for battery electrode manufacturing applications [2]. The cast lead alloy layer is in the UNS group L52900–L53099, usually has a high Sb content of about 3.5–5% to increase the hardness and durability of the battery electrodes. The hardness of the cast lead alloy layer after heat treatment usually reaches 16 HV [3]. However, the solidification behavior, phase constitution, and final properties of Pb–Sb-based alloys are strongly influenced by alloy

composition, casting route, and cooling rate [4-8] Therefore, the rapid cooling from liquid to solid state often results in an unbalanced microstructure, characterized by dendritic crystallization, high residual internal stress, high hardness, brittleness, susceptibility to microcracks, and high electrical resistance, together with microsegregation and structural heterogeneity that may accelerate damage during service [2, 4, 5, 7-11].

When working in highly corrosive, acidic environments, the microstructure of the lead alloy layer on the electrode tip must achieve equilibrium, have low residual internal stress to limit localised corrosion, and have low electrical resistance to avoid heat generation. Previous studies have shown that casting method, corrosion behaviour, failure characteristics, and natural or artificial aging can significantly influence the microstructure and mechanical performance of Pb–Sb and related lead battery alloys [5, 7-10]. Nevertheless, compared with conventional studies on bulk battery grids, there is still limited published information on the optimisation of heat treatment for a lead-alloy layer cast directly onto a copper electrode substrate, where metallurgical bonding, stress relief, structural equilibration, hardness, and through-layer electrical resistance must be controlled simultaneously [12-14].

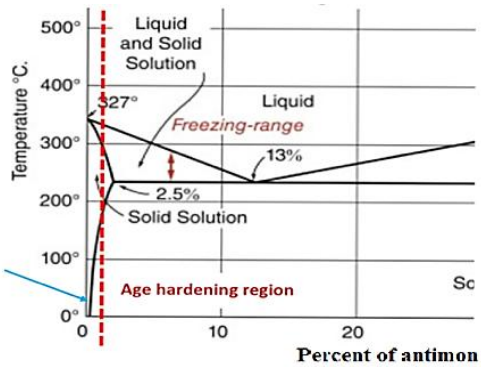

Figure 1. *Pb-Sb diagram and some electrode terminals of a high-capacity lead-acid battery [15].*

Research into the heat treatment of lead alloys used in high-capacity batteries is of great interest to manufacturers worldwide, as it aims to improve the mechanical properties of components and extend battery life. This paper presents research results on a heat-treatment method for cast lead-antimony alloy layers used in the fabrication of advanced high-capacity lead-acid battery terminals with anode spines made of a Pb-Sn-Ca alloy.

2. EXPERIMENTS AND RESEARCH METHODS

2.1. Research equipment and supplies

The equipment used included: a Lenton 1400 °C furnace from Germany, a graphite crucible from China, titanium or SUS316 steel stirring rods, a heated drying oven from Vietnam, an analytical balance from Japan, a metal cutting machine from the Netherlands, an IR-AHS0 remote temperature measuring device from Vietnam, a two-half cast iron mould, and cutting, grinding, and polishing machines from the Netherlands.

The experiments utilized the following materials: pure lead ingots Pb ≥ 99.97% from Vietnam, pure antimony ingots from Vietnam with Sb ≥ 99.75%, tin-lead alloy 60/40, technical grade pure copper 99.90%; acetic acid ($C_2H_4O_2$, PA, Germany), hydrogen peroxide (H_2O_2, PA, Germany), glycerol ($C_3H_8O_3$, PA, Germany), nitric acid (HNO_3, PA, Germany), argon gas with 99.995% purity.

2.2. Experiment

To create a lead-antimony alloy with approximately 5% Sb, the smelting is carried out in a Lenton furnace under argon gas protection. The furnace is set to 660 ºC, and a ceramic crucible made of aluminum oxide containing lead at a mass ratio of 94.75% is heated along with it. When

the lead is fully melted, antimony is added at a 5% ratio. The addition of antimony is divided into two stages: 2.5% is added each time, stirred for 1 minute, and then added again until the 5% is used up. The loss rate of Pb, Sb, and Sn in an inert gas environment during casting is approximately 0.5% [16]. The copper electrode is fixed in a two-half cast iron mould. The mould and copper electrode are heated to 200 ºC. After gravity casting, the specimens are removed from the mould at 100 °C. The specimens are then allowed to stabilize at room temperature for 24 hours before being tested for HV hardness, resistance from the cast lead alloy layer to the copper electrode, and the structure of the cast lead alloy.

Next, the samples were quenched at 200 °C, 220 °C, 240 °C, and 260 °C for 60 minutes each, then cooled in water to determine the optimal quenching temperature. After identifying the optimal quenching temperature, the aging process was investigated at 100 °C, 110 °C, and 120 °C for varying durations to achieve maximum hardness. The electrical resistance at each mode was also measured. For the aging mode that yielded the best mechanical properties, the samples were examined using optical microscopy for comparison and evaluation.

2.3. Research methods

The metal analysis methods used included: emission spectroscopy on a Metal Lab 75/80J MVU-GNR instrument (Italy); HV hardness measurement on a Duramin microhardness tester (Japan); metallographic microscopy on an Axio Image A2M optical microscope (Germany); and resistance measurements were taken on the Hioki BT 3554 series battery tester device with six defined measurement positions on the cast lead alloy layer up to a fixed position on the copper electrode tip (Japan).

3. RESULTS AND DISCUSSION

3.1. Microstructure characteristics, hardness, and electrical resistance of the lead alloy layer covering copper electrode manufactured by gravity casting

The results of the chemical composition analysis of the lead alloy layer on the copper electrode manufactured by gravity casting are shown in Table 1.

Table 1. *Chemical composition of the lead alloy layer on the copper electrode.*

Composition,%	Sn	Sb	Al	Bi	Cu	Fe	As	Pb
Lead alloy layer covering the electrode	0.2898	5.1803	0.0023	0.0032	0.0416	0.0010	0.0844	The rest

According to these results, the chemical composition of the lead alloy is equivalent to the US UNS L52922-L52930 lead-antimony alloy grade. The average hardness of the lead alloy is 27.9 ± 0.4 HV.

The microstructure of the samples was rough-ground, fine-ground, and polished, and the crystal boundaries were etched according to ASTM E407-07 using a solution of 75 ml acetic acid ($C_2H_4O_2$), 25 ml 30% concentrated hydrogen peroxide (H_2O_2), and 15 ml glycerol ($C_3H_8O_3$) for 15 minutes. They were then dried and cleaned with 70% concentrated nitric acid. The microstructure of the lead alloy layer in the cast state is shown in Figure 2.

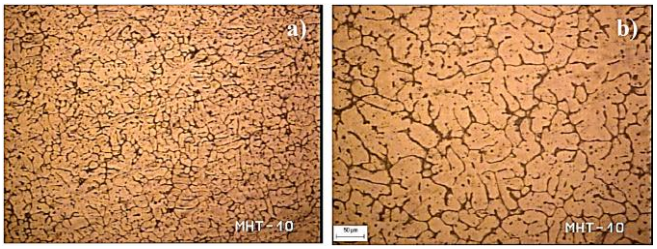

Figure 2. *Microstructure of the lead alloy layer in the cast state, 100x (a), 200x (b).*

According to the results in Figure 2, the microstructure of the cast alloy layer is dendritic. This is characteristic of an unbalanced structure, a high-energy state, so there is a large residual internal stress. When an external force is applied, the external stress, combined with the residual internal stress, can easily exceed the material's strength limit, leading to failure phenomena such as cracking and breaking [2]. Dendritic regions, when solidified from the liquid state, have the following characteristics: the first basic branch is richest in Pb, and the last branch has a lower Pb content [1]. The surrounding non-dendritic region is rich in Sb (after heat treatment, these regions often form grain and phase boundaries). The distance between the dendritic regions in Figures 2a and 2b is mainly less than 40 μm. The spacing of the branches and the degree of uniformity of that spacing will affect the crystal grain size during heat treatment. The smaller and more uniform the spacing, the finer the crystal grains, the less the tendency to crack, and the higher the mechanical properties of the material. In the field of heat treatment, the requirement is that the crystal grain size after heat treatment must not exceed the spacing between branches in the cast state. Only then will the microstructure be ensured not to be roughened [8].

Electrical resistance between the lead alloy surface and the copper electrode tip was measured for 3 samples, each tested at 3 locations. The results are shown in Table 2.

Table 2. *Resistance from the lead alloy surface to the copper electrode surface.*

Sample	Resistance (mΩ)			Average resistance (mΩ)
M1	0.415	0.425	0.420	0.420 ± 0.004
M2	0.310	0.304	0.322	0.312 ± 0.007
M3	0.354	0.365	0.403	0.374 ± 0.021

According to Table 2, the resistance from the surface of the lead alloy layer to the surface of the copper electrode for sample M1 was 0.420 mΩ; similarly, sample M2 was 0.312 mΩ, and sample M3 was 0.374 mΩ. This result can be explained by the fact that when the alloy is in a non-equilibrium phase state, a large amount of excess energy accumulates within the structure, and the defect density is also high. This non-equilibrium phase acts as a strong scattering centre, reducing the average electron free path and increasing resistivity. The electrode tip surface position is fixed; sample M2 is closest to the copper electrode tip, sample M1 is furthest, and sample M3 is located between samples M1 and M2. The farther the position is from the origin, the greater the resistance, and vice versa.

3.2. Microstructure characteristics, hardness, and electrical resistance of the lead alloy layer on copper electrode after heat treatment

The process of examining curing conditions at 200 °C, 220 °C, 240 °C, and 260 °C for 60 minutes, followed by cooling in water, produced the microstructure shown in Figure 3. The crystal structure partially transformed at 200 °C into polygonal crystal grains, though not very clearly (Figure 3a). Locally, some areas still showed traces of dendritic crystal structure, clearly indicating that residual internal stress had not been eliminated. Meanwhile, at higher quenching temperatures such as 220 °C (Figure 3b), 240 °C (Figure 3c), and 260 °C (Figure 3d), the crystal structure was completely polygonal. The crystal grain size was evaluated using the Planimetric method (ASTM E-112) by drawing three circles with a radius of 50 μm on the microstructure images in Figures 3b, 3c, and 3d. Grains completely inside the circles were multiplied by a factor of 1, and grains crossing the circles were multiplied by a factor of 1/2 [8]. The average particle size will be calculated through the average particle area recorded in Table 3.

According to the average particle size calculations in Table 3 and the microstructure image in Figure 3, it is evident that only in the heat-treated at 220 °C case is the crystal grain size uniform

in both dimensions, with very few grains larger than 40 µm. In contrast, when heat-treated at 240 °C and 260 °C, the microstructure image shows a relatively high proportion of crystal grains with one dimension greater than 50 µm. Some grains even reach 100 µm. This is due to the growth of crystal grains, according to the principle that larger grains engulf smaller grains under the influence of temperature. When heat-treated at 240 °C or higher, abnormal crystal growth is very likely.

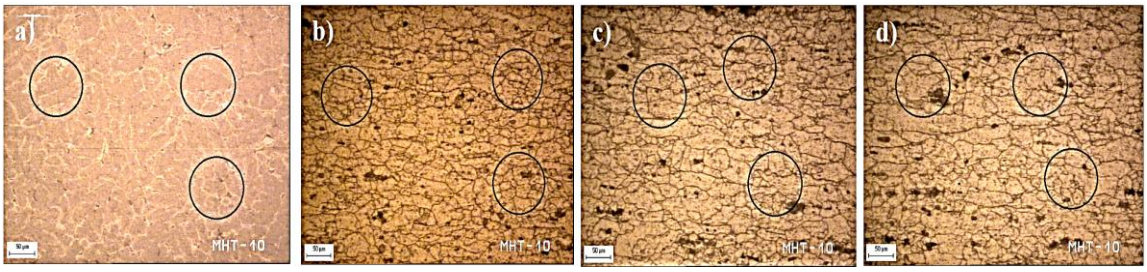

Figure 3. *Microstructure images of the lead alloy layer in the quenched state at temperatures of 200 °C (a), 220 °C (b), 240 °C (c), and 260 °C (d), 200x.*

Table 3. *Average particle size corresponding to different quenching temperatures.*

Quenching temperature (°C)	Average particle area (mm^2)	Average particle size (µm)
220	0.00081 ± 0,0000324	32.2 ± 0,644
240	0.00118 ± 0000472	38.8 ± 0,776
260	0.00147 ± 0,0000588	43.2 ± 0,864

The hardness and electrical resistance of the alloy layer after quenching were investigated, and the results are shown in Table 4.

Table 4. *Hardness and average electrical resistance of lead alloy grades corresponding to different quenching temperatures.*

Quenching temperature (°C)	Average hardness (HV)	Average resistance (mΩ)	Quenching temperature (°C)	Average hardness (HV)	Average resistance (mΩ)
200	17.4 ± 0.435	0.217 ± 0.0021	240	12.4 ± 0.31	0.189 ± 0.0019
220	13.1 ± 0.33	0.184 ± 0.0018	260	11.6 ± 0.29	0.175 ± 0.0017

The hardness at 200 °C remained quite high at 17.4 HV. Meanwhile, when the quenching temperature was sufficient to fully transform the microstructure from a dendritic crystal form to a polygonal crystalline grain form, the hardness was only 11.6-13.1 HV. Quenching at 220 °C ensured the most uniform polygonal crystalline grain microstructure, and the hardness remained relatively high at 13.1 HV. The higher the quenching temperature, the more likely abnormal crystal grain growth will occur, thereby reducing the alloy's hardness. Clearly, these results show that quenching at 200 °C indicates the microstructure has not completely transformed, so the residual internal stress has not been fully eliminated. Thus, the appropriate quenching temperature to create a supersaturated solid solution for the lead alloy coating on the copper electrode tip is 220 °C. The resistance of the samples in the post-cast state also decreased by about 50% compared to the cast state. After selecting a suitable temperature of 220 °C, the samples were examined for changes in microstructure and mechanical properties during aging at 90 °C, 100 °C, and 110 °C. The hardness and electrical resistance of the lead alloy coating on the copper electrode tip during aging at different temperatures are shown in Figure 4.

The hardness reached a maximum of 16.2 HV after aging at 110 °C for 7 hours. Extending the aging time tended to decrease hardness as the dispersed chemical phases clumped together, reducing the hardening effect. Aging at 100 °C yielded a maximum hardness of 15.7 HV for 9 hours. Aging at 120 °C yielded a maximum hardness of 16.1 HV for 6 hours. The resistance of the lead alloy coating on the copper electrode tip reached its maximum of 0.06 mω after 7 hours at 110 °C; further aging did not significantly change the resistance. Aging at 120 °C for 6 hours also resulted in a resistance of 0.061 mΩ. Furthermore, aging at 100 °C only ensured that the resistance reached 0.092 mΩ after the shortest processing time of 9 hours.

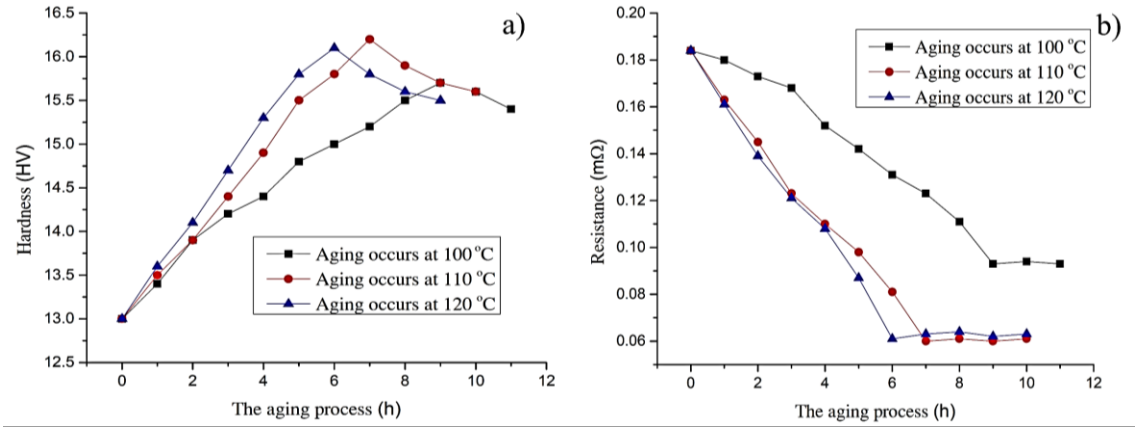

Figure 4. *Hardness (a) and electrical resistance (b) of the lead alloy layer during aging at temperatures of 100 °C, 110 °C, and 120 °C.*

The microstructure was investigated using phase-precipitation etching with approximately 30% etchant concentration at the grain boundaries. With this etching technique, the crystal grain boundaries were not corroded, but the antimony-rich β-phase precipitates were corroded first. The microstructure images of the lead alloy layer after quenching and after aging, corresponding to the conditions that yielded the best hardness and electrical resistance, are shown in Figure 5.

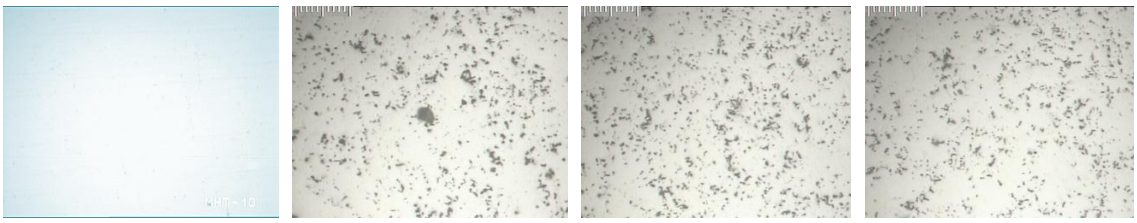

a) *b)* *c)* *d)*

Figure 5. *Microstructure of the lead alloy layer after quenching (a), after aging at 100 °C (b), 110 °C (c), 120 °C (d), 200x.*

The microstructure image after quenching in Figure 5a does not show dispersed stabilized phase precipitates. This is because in the quenching state, antimony dissolves into the supersaturated α-Pb solid solution matrix. When heat-treated at the temperatures and times investigated above, phase precipitates formed with varying degrees of dispersion and size. Aging at 100 °C (Figure 5b) did not show the stabilized phases as in the cases of aging at 110 °C (Figure 5c) and 120 °C (Figure 5d). Aging at 110 °C clearly showed the best dispersion. The EDS spectra of the β-phase secretion region and the region surrounding the secretion site are shown in Figure 6.

EDS analysis results show that the region surrounding the phase-secreting site (Figure 6a) has a lower Sb ratio than the phase-secreting region (Figure 6b). This demonstrates the formation of a phase aging effect: an antimony-rich region and an antimony-poor region.

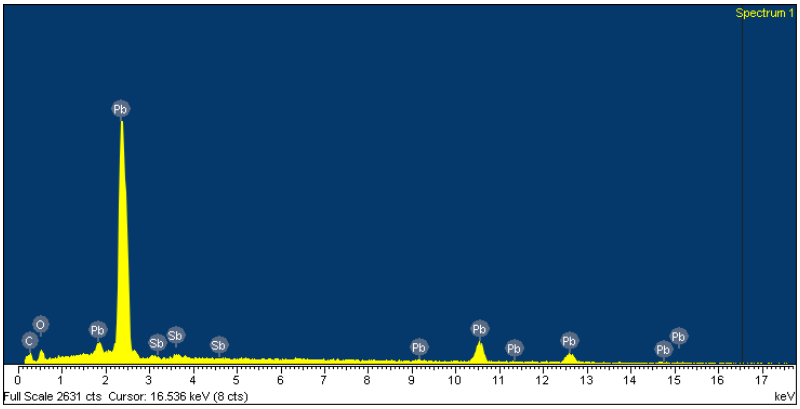

Element	Weigh%
C K	5.07
O K	9.96
Sb L	2.25
Pb M	82.72
Totals	100.00

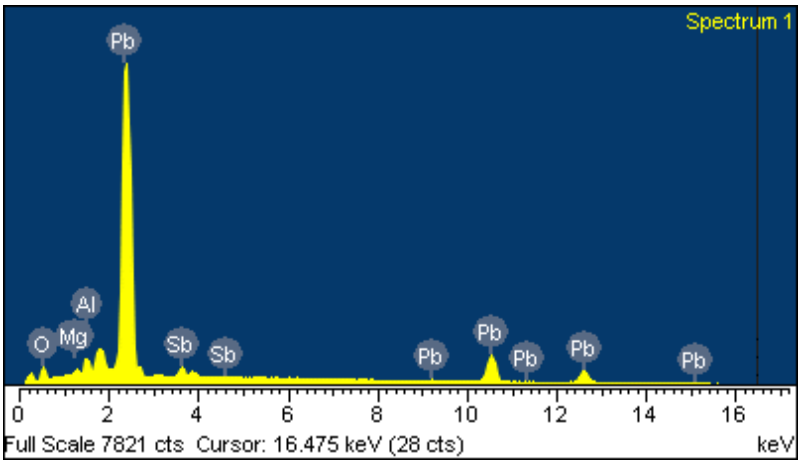

Element	Weigh%
O K	9.69
Mg K	0.57
Al K	1.83
Sb L	5.4
Pb M	82.51
Totals	100.00

Figure 6. *EDS spectrum of the β-phase secretion region (b) and the region surrounding the secretion site (a).*

4. CONCLUSIONS

Using heat treatment technology, including quenching at 220 °C for 60 minutes and aging at 110 °C for 7 hours, the lead alloy coating on the copper electrode tip, which previously had an unbalanced dendritic crystal structure (high residual internal stress, high hardness of 27.9 HV; high resistance of 0.312 ÷ 0.420 mΩ), transformed into a balanced structure with polygonal, axially equal crystals. The hardness remained high at 16.2 HV, and the resistance was reduced to 0.06 mω, making it well suited for the manufacture of advanced high-capacity lead-acid batteries.

Acknowledgment: *The authors appreciate financial support from the project NCUD.04-2025.18.*

REFERENCES

[1]. Davis, J. R., "*Metals Handbook Desk Edition*", ASM International, (1998).
[2]. Ha, N. D., Nguyen, T. H. D., Doan, T. A., Doan, M. C. and Vu, M. T., "*Investigation of the effects of heat treatment on the microstructure and mechanical properties of Pb-Sb alloy used in fabrication of anode spines for high-capacity lead-acid batteries*", Journal of Military Science and Technology, Vol. 105, pp. 60–66, (2025).
[3]. Pavlov, D., "*Lead-acid batteries: Science and technology*", 2nd ed., Elsevier, (2017).
[4]. Ali, E. et al., "*Effects of Sb and/or Sn concentrations on the SbSn formation in a ternary melt-spun Pb-Sb-Sn alloy*", Results in Materials, Vol. 16, p. 100307, (2022).
[5]. Dzenzerskiy, V. O., Tarasov, S. V., Sukhova, E. V. and Ivanov, V. A., "*Evolution of Mechanical Properties of Pb–Sb–Sn–As–Se Grid Alloys for Lead-Acid Batteries during Natural Aging*", East European Journal of Physics, No. 4, pp. 182–188, (2023).

[6]. Ku, B.-K. and Jeong, S.-W., "*A Study on the Pb-Ca-Sn Grid Alloy of Positive Plate in Lead-Acid Battery*", Journal of the Korean Applied Science and Technology, Vol. 25, No. 4, pp. 518–524, (2008).
[7]. Seikh, A. H. et al., "*Microstructure characterization and corrosion resistance properties of Pb-Sb alloys for lead acid battery spine produced by different casting methods*", PLoS One, Vol. 13, No. 4, p. e0195224, (2018).
[8]. Tariq, F., Azher, S. U. and Naz, N., "*Failure analysis of cast lead–antimony battery grids*", Journal of Failure Analysis and Prevention, Vol. 10, No. 2, pp. 152–160, (2010).
[9]. Prengaman, R. D., "*Challenges from corrosion-resistant grid alloys in lead acid battery manufacturing*", Journal of Power Sources, Vol. 95, No. 1–2, pp. 224–233, (2001).
[10]. Rocca, E., Bourguignon, G. and Steinmetz, J., "*Corrosion management of PbCaSn alloys in lead-acid batteries: Effect of composition, metallographic state and voltage conditions*", Journal of Power Sources, Vol. 161, No. 1, pp. 666–675, (2006).
[11]. Pavlov, D., Dimitrov, M., Rogachev, T. and Bogdanova, L., "*Influence of paste composition and curing program used for the production of positive plates with PbSnCa grids on the performance of lead acid batteries*", Journal of Power Sources, Vol. 114, No. 1, pp. 137–159, (2003).
[12]. Saravanan, M. and Ambalavanan, S., "*Failure analysis of cast-on-strap in lead-acid battery subjected to vibration*", Engineering Failure Analysis, Vol. 18, No. 8, pp. 2240–2249, (2011).
[13]. Wang, E., Shi, P. and Gao, J., "*Research on thin grid materials of lead-acid batteries*", Rare Metals, Vol. 25, No. 6, Supplement 1, pp. 43–46, (2006).
[14]. Dzenzerskiy, V., Tarasov, S., Sukhova, O. V. and Ivanov, V., "*Effects of Composition and Cooling Rate on Mechanical Properties of Pb-Sb-Sn-As Grid Alloys*", Romanian Journal of Physics, Vol. 69, p. 605, (2024).
[15]. Ruetschi, P., "*Review on the lead—acid battery science and technology*", Journal of Power Sources, Vol. 2, No. 1, pp. 3–120, (1977).
[16]. Worcester, A. W. and O'Reilly, J. T., "*Lead and Lead Alloys*", ASTM Handbook, Vol. 2, Properties and Selection: Nonferrous Alloys and Special-Purpose Materials, pp. 1655–1693, (1992).
[17]. Torralba, M., Aballe, M. and Regidor, J. J., "*Ageing behaviour of cast Pb-Sb battery grids*", Journal of Power Sources, Vol. 4, pp. 53–64, (1979).

TÓM TẮT

Nghiên cứu đặc tính chuyển biến tổ chức tế vi và cơ lý tính của lớp hợp kim chì bọc đầu điện cực đồng ắc quy chì-axit dung lượng cao khi xử lý nhiệt

Lớp hợp kim chì bọc bên ngoài điện cực đồng của ắc quy chì-axit dung lượng cao được chế tạo bằng phương pháp đúc trọng lực. Lớp hợp kim chì khi ở trạng thái đúc có tổ chức tế vi dạng tinh thể nhánh cây, không cân bằng, độ cứng cao 27,9 HV, nội ứng suất dư lớn nên dễ phát sinh vết nứt tế vi và điện trở lớn 0,312 ÷ 0,420 mΩ, không có lợi cho ắc quy. Bằng công nghệ xử lý nhiệt gồm tôi ở 220 ºC thời gian 60 phút, kết hợp với hóa già ở 110 ºC thời gian 7 giờ, tổ chức tế vi trạng thái đúc đã chuyển biến sang dạng hạt tinh thể đa cạnh, đều trục, cân bằng hơn, tiết pha hóa bền phân tán đã được hình thành, độ cứng tối ưu đạt 16,2 HV, điện trở trung bình giảm xuống còn 0,06 mΩ, phù hợp cho chế tạo ắc quy chì-axit dung lượng cao.

Từ khóa: Ắc quy chì-axit dung lượng cao; Hợp kim điện cực; Tổ chức tế vi; Độ cứng; Xử lý nhiệt.